Enantioselective photocatalytic synthesis of bicyclo[2.1.1]hexanes as *ortho*-disubstituted benzene bioisosteres with improved biological activity

Pablo Garrido-García,[1] Irene Quirós,[1] Paula Milán-Rois,[2] Álvaro Somoza,[2] Israel Fernández,[3,4] Thomas Rigotti[,1] and Mariola Tortosa*[,1,4,5]*

[1] *Department of Organic Chemistry, Faculty of Science, Autonomous University of Madrid, 28049 Madrid, Spain.*

[2] *IMDEA Nanociencia, 28049 Madrid, Spain.*

[3] *Department of Organic Chemistry, Faculty of Chemistry, Complutense University of Madrid, 28040 Madrid, Spain.*

[4] *Center of Innovation in Advanced Chemistry (ORFEO-CINQA).*

[5] *Institute for Advanced Research in Chemical Sciences (IAdChem), Autonomous University of Madrid, 28049 Madrid, Spain.*

1,5-Disubstituted bicyclo[2.1.1]hexanes are bridged scaffolds with well-defined exit vectors that are becoming increasingly popular building blocks in medicinal chemistry since they are saturated bioisosteres of *ortho*-substituted phenyl rings. Here we have developed the first enantioselective catalytic strategy based on a Lewis acid-catalyzed [2+2] photocycloaddition to obtain these motifs as enantioenriched scaffolds, providing an efficient approach for their incorporation in a variety of drug analogues. The bioisostere-containing drugs have been evaluated in cancer cell viability studies, observing that in some cases the biological activity of the two enantiomers is highly different. This showcases that the control of the absolute configuration and tridimensionality of the drug analogue has a large impact on its bioactivity, highlighting the need for stereoselective methods towards the construction of the bicyclo[2.1.1]hexane core.

Introduction

The benzene ring is a prevalent motif found in many marketed drugs, being one of the building blocks for the assembly of molecules in drug discovery programs.[1] This is essentially due to the availability of efficient and complementary methods for the construction of carbon-carbon bonds involving C(sp^2) atoms, in comparison with the incorporation of saturated analogues.[2] Although in some cases the benzene ring contained in the drug skeleton is essential for the establishment of crucial hydrophobic interactions within the enzyme pockets of biological systems,[3,4] in other cases, this aromatic scaffold is only acting as a linker that connects different functional group-containing fragments.[5] In this context, the benzene substitution pattern and the corresponding exit vectors play a decisive role in the construction of the overall molecular architecture, determining the specific spatial orientation of the drug, which can lead to an efficient interaction with the corresponding receptors in biological systems. Nevertheless, in the last decades, an increasing interest in the use of small F(sp^3)-rich scaffolds in drug discovery programs has fostered chemists towards the development of sp^3-hybridized bioisosteres of two-dimensional aromatic cores.[6,7] Indeed, the replacement of the flat scaffolds that are routinely employed in the pharmaceutical industry with rigid three-dimensional motifs that have well-defined exit vectors can lead to a modulation of the biological and physicochemical properties of the drug candidate, such as its potency and metabolic stability, besides circumventing patent restrictions.[8]

The replacement of a phenyl ring for a saturated scaffold which mimics its substitution pattern was disclosed for the first time by Pellicciari and coworkers in 1996 through the introduction of a bicyclo[1.1.1]pentane moiety as an appropriate bioisostere of *para*-substituted arenes (Figure 1a).[9] Since then, different strategies have been developed for the incorporation of similar structures into drug-like molecules, establishing a variety of possible bioisosteres of *para*-substituted phenyl rings.[11-20] On the other hand, suitable bridged bicyclic scaffolds that mimic the exit vectors of *ortho*- and *meta*-substituted phenyl rings have been identified only recently. In this context, the pioneering report of Mykhailiuk and coworkers demonstrated that 1,5-disubstituted bicyclo[2.1.1]hexanes are suitable bioisosteres of *ortho*-substituted aromatic rings.[21] The sp^3-hybridized scaffolds were obtained through a racemic approach and validated as bioisosteres through the determination of their physicochemical properties, X-ray crystallographic analysis, and by the evaluation of two agrochemical derivatives as antifungal compounds. Moreover, motivated by the existing gap in the literature, several groups have explored novel activation modes and strategies to prepare non-linear bridged skeletons as possible analogues of *ortho*- and *meta*-substituted aromatic rings.[22-45] While scaffolds that mimic *para*- and *meta*-substituted benzenes shown in Figure 1 represent non-chiral building blocks, bioisosteres of *ortho*-substituted derivatives are chiral structures, including 1,2- and 1,5-disubstituted bicyclo[2.1.1]hexanes (1,2-BCH and 1,5-BCH, Figure 1b) and 1,2-difunctionalized bicyclo[1.1.1]pentanes (1,2-BCP, Figure 1b). Therefore, their synthesis involves an additional level of complexity since both the diastero- and the enantioselectivity need to be controlled. In the context of drug discovery, the development of enantioselective strategies that enable access to both enantiomers is an essential task, as they often display different behaviors in biological systems.[46] Nevertheless, despite the increasing interest of the scientific community in this field, there is currently a lack of enantioselective catalytic methodologies for the construction of these bicyclic skeletons. Herein, we disclose the first enantioselective catalytic strategy to obtain enantioenriched 1,5-disubstituted bicyclo[2.1.1]hexanes through a Lewis acid-catalyzed intramolecular crossed [2+2] photocycloaddition. The developed methodology has enabled

the incorporation of enantioenriched sp^3-hybridized bioisosteres into the structure of marketed drugs to prepare different drug analogues. Remarkably, in some cases, the biological activity of the enantiopure bioisosteres was significantly higher compared to the original sp^2-based structure, which was further modulated by the absolute configuration of the corresponding bioisosteres.

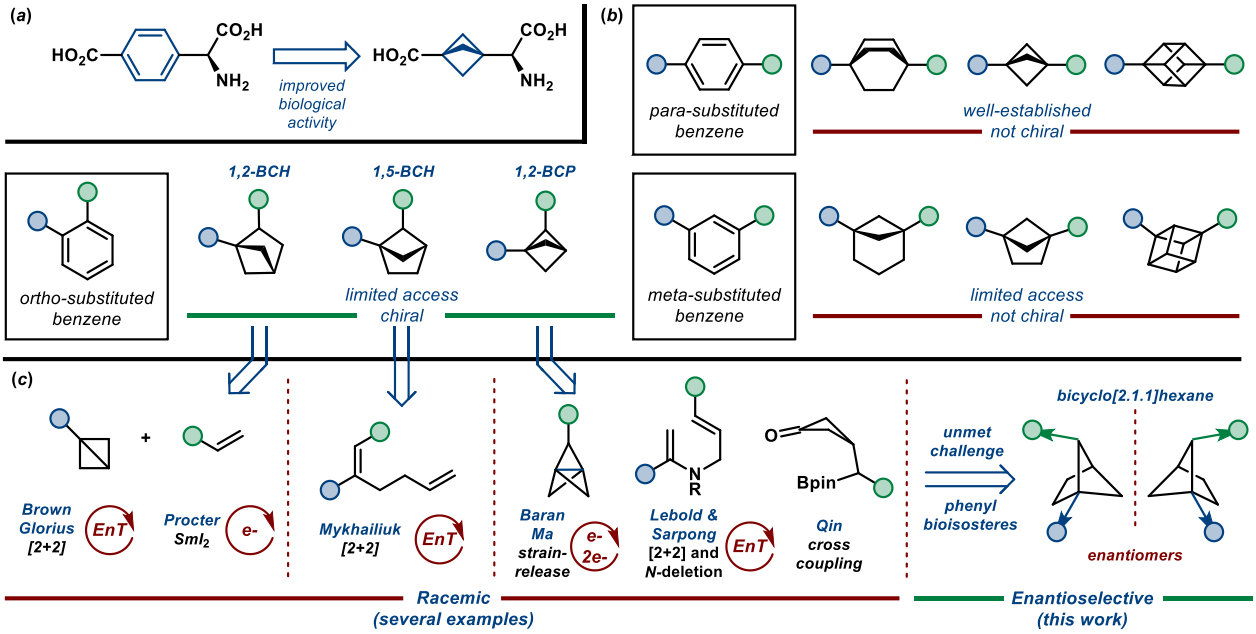

Figure 1 | Bridged bicyclic structures as bioisosteres of disubstituted phenyl rings. (*a*) Seminal report by Pellicciari on the incorporation of a bicyclo[1.1.1]pentane into a bioactive molecule. **(*b*)** Established bioisosteres of *para*-disubstituted benzenes and validated or suggested bioisosteres for *meta*- and *ortho*-disubstituted benzenes. **(*c*)** State-of-the-art strategies for the construction of bridged skeletons as *ortho*-phenyl bioisosteres and representation of the exit vectors of the 1,5-disubstituted bicyclo[2.1.1]hexane core.

Results and discussion

Design

Due to our interest in the development of enantioselective strategies for the synthesis of strained, conformationally rigid hydrocarbons as medicinal chemistry-relevant structures,[47-51] we wondered if it would be possible to establish a convenient preparation of enantioenriched 1,5-disubstituted bicyclo[2.1.1]hexanes. From the outset, we aimed to prepare bifunctional building blocks with two versatile and highly modulable handles that would allow easy incorporation into drug analogues. We turned our attention towards the use of visible light photocatalysis as a powerful activation mode that can enable bond formation that would not be possible to achieve by conventional thermal catalysis.[52,53] Inspired by the work of Mykhailiuk, we decided to rely on an intramolecular crossed [2+2] photocycloaddition[54] for the construction of the bioisostere skeleton, and we looked at the possibility of using Lewis acid catalysis for the activation of the substrate,[55,56] enabling a stereocontrolled reaction (Scheme 1). Specifically, we focused our efforts on the use of a chiral-at-rhodium catalyst developed by Meggers and coworkers,[57,58] which is a highly efficient Lewis acid catalyst that has been employed in a variety of asymmetric photocatalytic transformations. This catalyst seemed ideal for the establishment of a bidentate coordination with highly versatile and easily removable acyl pyrazole moieties, enabling further post-functionalization of the bicyclic products.[59-64] The Lewis acidic chiral-at-rhodium catalyst is expected to bind to the acyl pyrazole moiety to form a Lewis acid-substrate complex that will be capable of absorbing visible light to reach a triplet excited state from which the

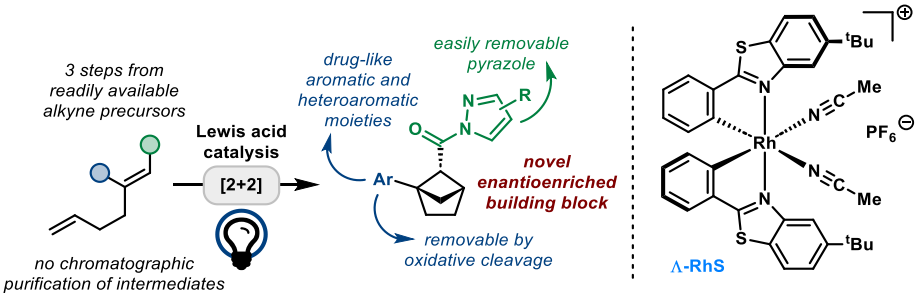

Scheme 1 | Envisioned strategy and requirements for the construction of versatile bridged structures as suitable bioisosteres of disubstituted phenyl rings. Synthesis of 1,5-disubstituted bicyclo[2.1.1]hexanes through an enantioselective intramolecular crossed [2+2] photocycloaddition catalyzed by a rhodium-based Lewis acid.

stereocontrolled [2+2] photocycloaddition can take place (*vide infra*). A convenient synthesis of the appropriate bicyclic precursors has been identified (see Supporting Information for details), enabling their preparation from readily available starting materials without any chromatographic purification and isolation of the corresponding reaction intermediates. In addition, we aimed at the development of a stereoconvergent process to circumvent any issues associated with the geometry of the starting α,β-unsaturated acyl pyrazole, and the unavoidable *E*/*Z*-isomerization that would be observed under irradiation.

Method optimization

We began our investigations with the model substrates (*E*)-**1a** and (*Z*)-**1a** as geometrical isomers of the same α,β-unsaturated acyl pyrazole. The use of a 4 mol% of **Λ-RhS** as the Lewis acid catalyst and dichloromethane as the solvent under blue LED (λ = 440 nm) irradiation afforded product **2a** in 91% yield and 95:5 *er* (Table 1, entries 1-2). Both (*E*)- and (*Z*)-isomers proved to be suitable starting materials, which afforded the same result and indicated that a stereoconvergent process was taking place. After a preliminary optimization screening in which the catalyst loading and the solvent were varied (see Supporting Information for details), the best result was obtained with a 2 mol% of Lewis acid and acetone as solvent, delivering product **2a** as a single diastereoisomer in 94% yield and 95:5 *er* (Table 1, entries 3-4). To further increase the enantioselectivity of the [2+2] photocycloaddition, we decided to prepare and test a series of α,β-unsaturated acyl pyrazoles that present different substitutions on the pyrazole ring. While no substitution or mono-substitution proved to be detrimental to the enantioselectivity (Table 1, entries 5-8), the introduction of two phenyl rings (pyrazole **1g**) afforded product **2g** in 97% yield and 98:2 *er* (Table 1, entry 10). Increasing the reaction scale to 0.1 mmol provided similar results, and we observed that the presence of oxygen did not have an impact on yield and stereoinduction, obtaining product **2g** as a single diastereoisomer in 96% yield and 98:2 *er* (Table 1, entry 12). Finally, the reaction did not proceed in the absence of catalyst or without light irradiation (Table 1, entries 13-14), indicating that both components are necessary to enable the photochemical reaction.

Table 1 | Optimization studies. Screening of reaction conditions and evaluation of the most effective pyrazole coordinating group.

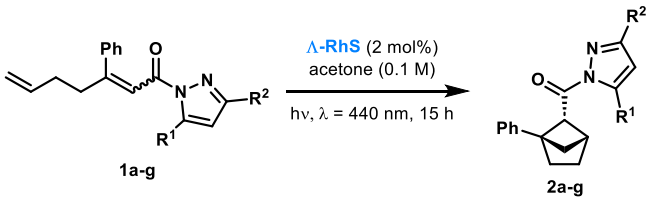

entry	isomer	R^1	R^2	conversion %	product	yield %	*er*
1[a]	(*E*)	Me	Me	100	**2a**	91	95:5
2[a]	(*Z*)	Me	Me	100	**2a**	91	95:5
3	(*E*)	Me	Me	100	**2a**	94	95:5
4	(*Z*)	Me	Me	100	**2a**	94	95:5
5	(*Z*)	H	H	100	**2b**	97	84:16
6	(*Z*)	H	Me	84	**2c**	n.d.	83:17
7	(*Z*)	H	*i*Pr	91	**2d**	n.d.	83:17
8	(*Z*)	H	Ph	100	**2e**	92	89:11
9	(*Z*)	*i*Bu	*i*Bu	67	**2f**	n.d.	88:12
10	(*Z*)	Ph	Ph	100	**2g**	97	98:2
11[b]	(*Z*)	Ph	Ph	100	**2g**	96	98:2
12[b,c]	(*Z*)	Ph	Ph	100	**2g**	96	98:2
13[d]	(*Z*)	Ph	Ph	0	-	-	-
14[e]	(*Z*)	Ph	Ph	0	-	-	-

The reactions were performed on a 0.05 mmol scale. Conversions were determined by ^{1}H NMR analysis. The yields refer to isolated material after purification by flash chromatography. [a] 4 mol% catalyst loading and dichloromethane as the solvent. [b] The reactions were performed on a 0.10 mmol scale. [c] The reaction was performed in the presence of air. [d] The reaction was performed without catalyst. [e] The reaction was performed in the dark. *n.d.* = not determined.

Scope of the method

With the optimized conditions in hand (entry 12, Table 1) the scope of the reaction was evaluated (Scheme 2). Different substitutions of the arene moiety such as *p*-Me (**2h**), *m*-Me (**2i**) and even the more sterically demanding *o*-Me (**2j**) or *p*-*t*Bu (**2k**) were tolerated, affording the products in high yields and enantioselectivities. Halogen atoms such as fluorine (*p*-F)

and chlorine (*p*-Cl) led to the corresponding products **2l** and **2m**. The presence of electron-donating (*p*-OMe) and electron-withdrawing substituents (*p*-CF_3 and *p*-NO_2) could be tolerated, obtaining products **2n**, **2o** and **2p** in high yields and enantioselectivities. Furthermore, extended aromatic systems, electron-poor, and electron-rich heteroaromatic moieties could be incorporated in the enantioenriched 1,5-disubstituted bicyclo[2.1.1]hexanes to deliver products **2q**, **2r** and **2s**. In addition, it is also important to mention that the reaction could be easily scaled to 1.0 mmol obtaining product **2g** in quant. yield and 98:2 *er*. Despite the generality of the process regarding the substitution on the arene, we encountered some limitations. As expected, the reaction of β-alkyl disubstituted acyl pyrazole **1t** did not provide any bicyclo[2.1.1]hexane and the starting material was recovered unaltered even upon irradiation at shorter wavelengths (λ = 390 nm). This is presumably

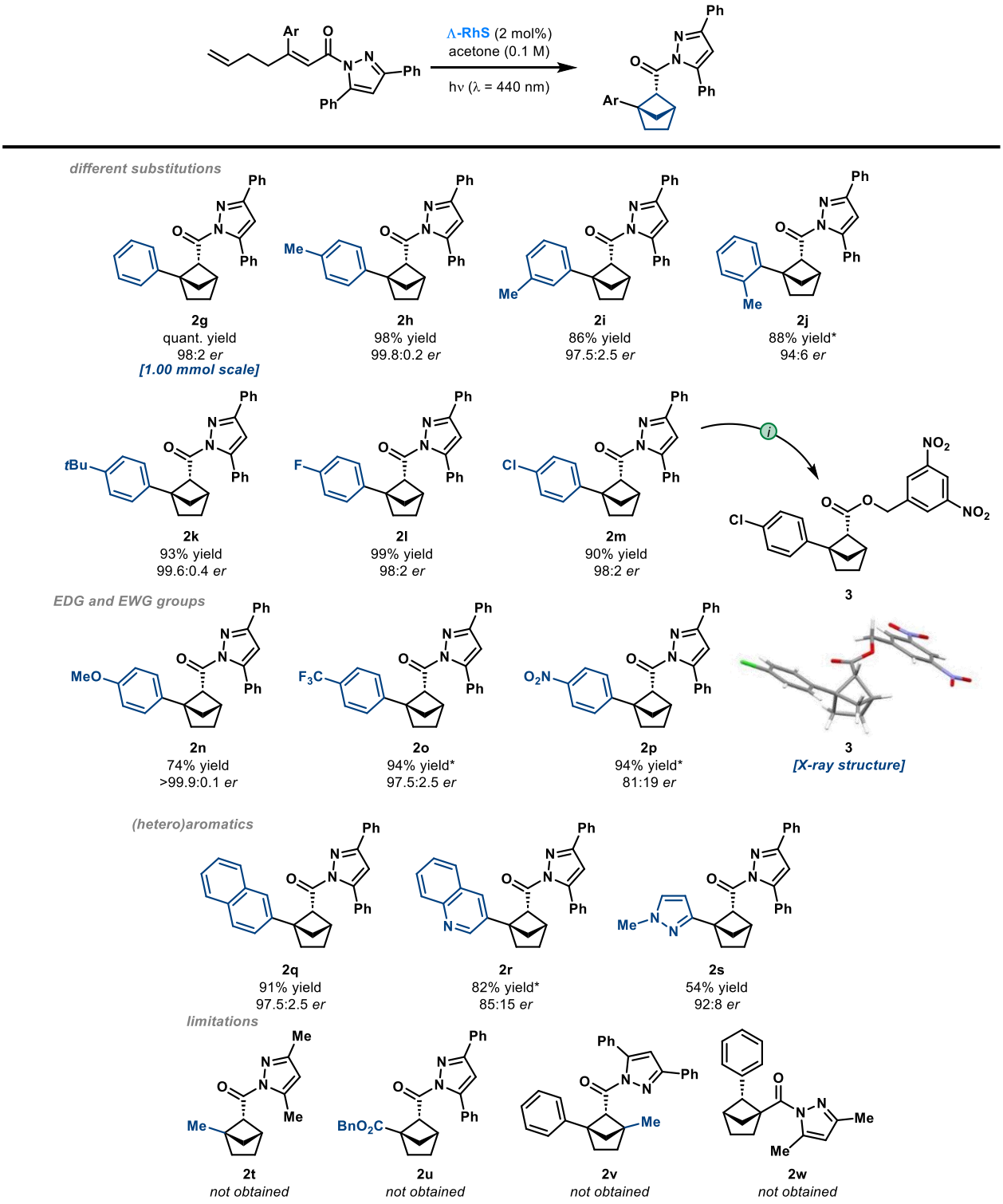

Scheme 2 | **Evaluation of the reaction scope.** Preparation of differently substituted enantioenriched 1,5-disubstituted bicyclo[2.1.1]hexanes by a Lewis acid-catalyzed crossed [2+2] photocycloaddition. The reactions were performed on a 0.10 mmol scale. * 5 mol% of catalyst loading was employed. [i] $LiOH{\cdot}H_2O$, THF-H_2O; then 3,5-dinitrobenzylalcohol, DCC, DCM. See S.I. for details.

due to deactivation pathways of the excited Lewis acid-substrate complex, which led to a relaxation of the excited species before any photocycloaddition could take place.[54] The same result was obtained with an α,β-unsaturated acyl pyrazole **1u** in which the aromatic ring was replaced by an ester group. A substrate with a tethered trisubstituted alkene (**1v**) only provided a mixture of unidentified products, while the use of a different substitution pattern on the olefin of the α,β-unsaturated acyl pyrazole scaffold (α-disubstitution) led to the recovery of the starting material **1w**. Finally, the absolute configuration of the enantioenriched 1,5-disubstituted bicyclo[2.1.1]hexanes could be established by X-ray crystallographic analysis of a 3,5-dinitrobenzyl ester derivative (**3**) of compound **2m** that was obtained through easy removal of the pyrazole moiety, followed by esterification.[65]

Incorporation into bioactive molecules

To validate a building block as a suitable bioisostere of *ortho*-disubstituted phenyl rings it is necessary to demonstrate that its incorporation into bioactive molecules and marketed drugs is feasible in a practical way. For these reasons, the bridged bicyclic structure must present suitable synthetic handles that allow their subsequent functionalization and manipulation. The acyl pyrazole moiety in compounds **2** complies with this criterion since it can be easily manipulated and removed, whereas electron-neutral or electron-rich arenes can be transformed into carboxylic acid derivatives by ruthenium-catalyzed oxidative cleavage (Scheme 1). Thus, we decided to carry out the enantioselective synthesis (Scheme 3) of the corresponding enantioenriched sp^3-hybridized drug analogues of a variety of marketed drugs that contain an *ortho*-disubstituted phenyl ring (Figure 2).

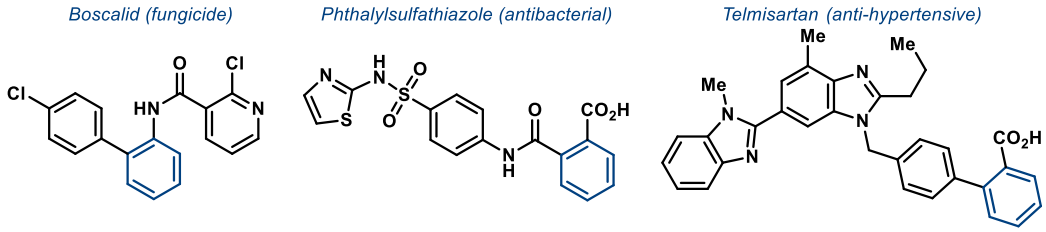

Figure 2 | **Targeted agrochemicals and drugs.** Chemical structures of the targeted agrochemicals and marketed drugs that contain an *ortho*-disubstituted phenyl scaffold.

We decided to start with the synthesis of the bicyclo[2.1.1]hexane-containing analogue **5** of the fungicide *Boscalid*, which was easily obtained in three steps from **2m** by a sequence of hydrolysis, Curtius rearrangement and acylation reaction (*er* of **5** = 98:2). Next, we identified bifunctional building block **7** as an intermediate for the preparation of *Phthalylsulfathiazole* sp^3-analogue **9** (Scheme 3). Enantiomerically enriched **7** was easily prepared from **2g** by a sequence of esterification and ruthenium-catalyzed oxidative cleavage of the aromatic ring. From **7**, amide bond formation and subsequent saponification provided **9** in excellent yield (*er* = 98:2). In addition, the absolute configuration of the sp^3-hybridized *Phthalylsulfathiazole* methyl ester **8** could be established by X-ray crystallographic analysis.[66] Moreover, simple manipulation of the carboxylic acid functional group of **7** could provide the bifunctional building block **10** which contains a redox active ester moiety and that could be employed as a synthetic handle for further functionalization. In the end, the last analogue that was investigated was the one that would mimic the antihypertensive drug *Telmisartan*. Compound **17** was obtained starting from enantioenriched compound **2h** by a sequence of esterification, radical bromination, nucleophilic substitution by the nitrogen-containing heteroaromatic scaffold, and final saponification of the ester moiety (*er* of **17** = 99.8:0.2).

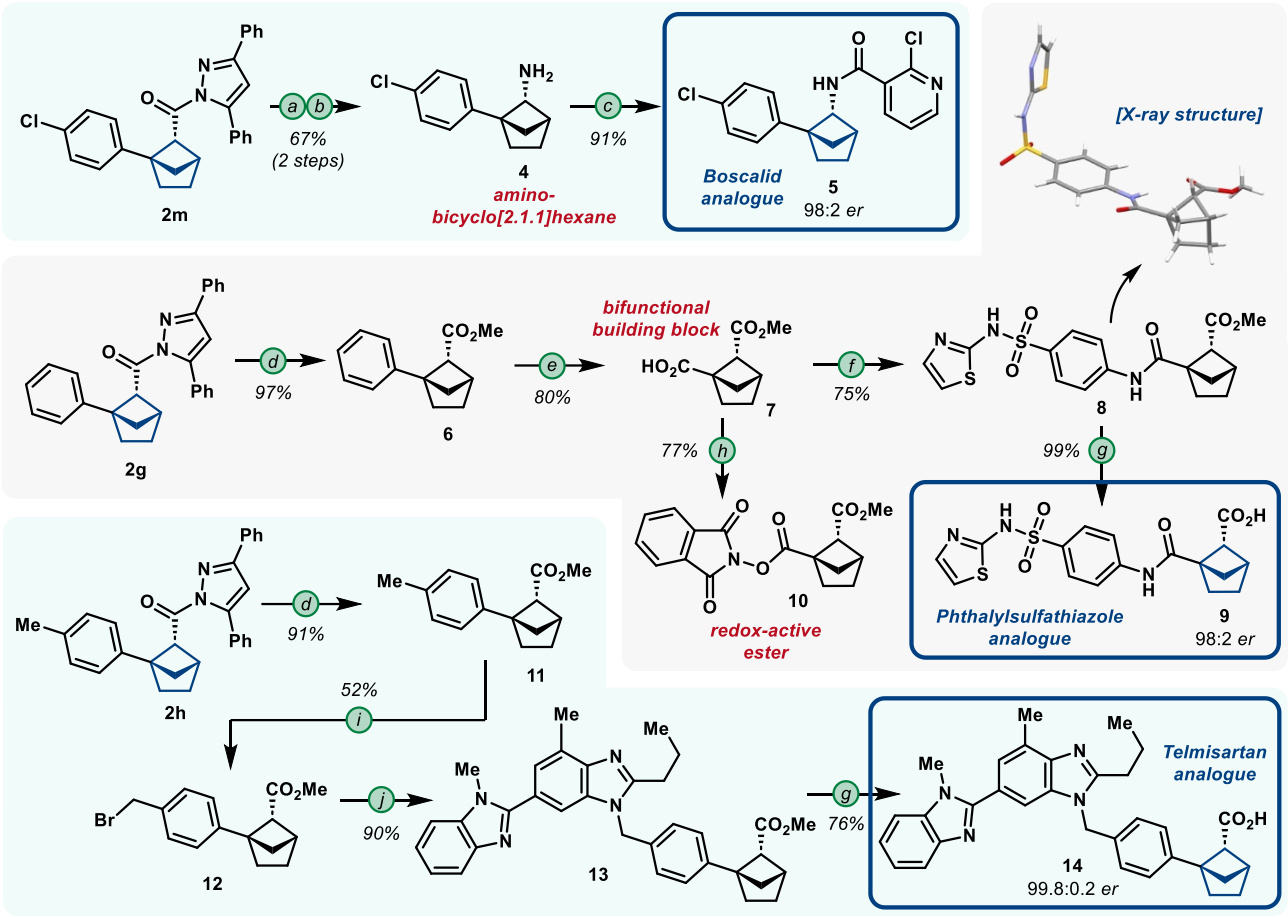

Scheme 3 | **Preparation of the bioisostere-containing drug analogues.** Derivatization of the enantioenriched compounds to prepare drug analogues with the 1,5-disubstituted bicyclo[2.1.1]hexane core. (*a*) $LiOH{\cdot}H_2O$, THF-H_2O. (*b*) DPPA, Et_3N, toluene, 85 ºC; then THF, NaOH, rt. (*c*) 2-Chloronicotinic acid, oxalyl chloride, DMF (cat.), DCM; then bicyclo[2.1.1]hexane-amine **4**, Et_3N, 0 ºC to rt. (*d*) LiCl, Et_3N, THF-MeOH. (*e*) $RuCl_3{\cdot}xH_2O$, $NaIO_4$, MeCN-DCM-H_2O. (*f*) Oxalyl chloride, DMF (cat.), DCM; then sulfathiazole, Et_3N, 0 ºC to rt. (*g*) NaOH, MeOH (reflux). (*h*) Oxalyl chloride, DMF (cat.), DCM; then *N*-hydroxyphthalimide, Et_3N, DMF, 0 ºC to rt. (*i*) NBS, AIBN, CCl_4 (reflux). (*j*) 2-*n*-Propyl-4-methyl-6-(1-methylbenzimidazole-2-yl)benzimidazole, NaH, DMF, 0 ºC to rt. See S.I. for details.

Biological Studies

1,5-Disubstituted bicyclo[2.1.1]hexanes have been recently validated as suitable bioisosteres of the phenyl ring, providing similar physicochemical properties to the corresponding sp^3-hybridized analogues.[21] Nevertheless, as highlighted by the corresponding exit vectors, due to the inherent tridimensionality and chirality of the 1,5-disubstituted bicyclo[2.1.1]hexane core (Figure 1), its absolute configuration determines the overall shape and molecular architecture of a specific drug analogue, enabling a different interaction of the two enantiomers in biological complex systems. As a consequence, since our developed methodology allowed the construction of three bicyclo[2.1.1]hexane-containing drug analogues (**5**, **9**, and **14**) in a stereocontrolled manner, we decided to evaluate the biological activity of the two enantiomers, in line with the regulations on chiral drugs of the FDA and EMA.[46] Thus, cell viability studies have been conducted with both enantiomers of the sp^3-hybridized molecules in different cancer cell lines and compared to the marketed sp^2-drugs (Figure 3).

Although *Boscalid* and *Telmisartan* showed similar behavior compared to their corresponding enantioenriched sp^3-analogues, this was not the case for *Phthalylsulfathiazole* (Figure 3). As can be observed, the saturated analogues of *Phthalylsulfathiazole* exhibited higher toxicity than the sp^2-drug, showcasing that the replacement of a flat scaffold for a tridimensional one can lead to higher activity. Specifically, *ent*-**9** exhibited a 2.2-fold higher toxicity than the sp^2-drug. Furthermore, even more relevant was the comparison of the saturated enantiomers. Thus, the sp^2-based marketed drug *Phthalylsulfathiazole* and the bioisostere-containing analogues **9** and *ent*-**9** were evaluated in three different cell lines: breast cancer cell line MB231, uveal melanoma cell line Mel202 and colon cancer cell line HCT116 (Figure 4 and Supporting Information for further details). The results corroborated not only a different drug sensitivity among the cell lines but also a different behavior of the two enantiomers in biological systems. Indeed, the highest difference was observed in the uveal melanoma cell line Mel202. The toxicity of compound **9** was 3.9-fold higher than marketed *Phthalylsulfathiazole* and 3.6-fold higher than *ent*-**9** (Figure 4B). This indicates that the absolute configuration of the bioisostere core plays a crucial role in determining its bioactivity and highlights the importance of developing an enantioselective catalytic strategy for the obtainment of these building blocks.

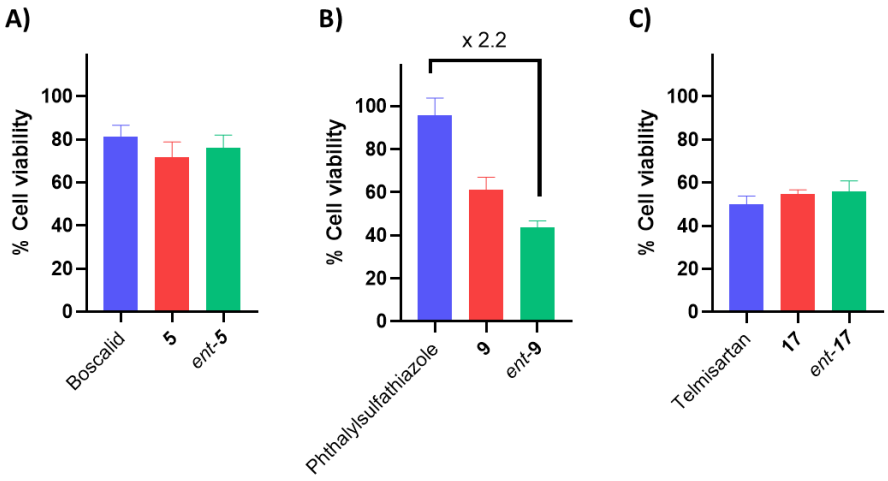

Figure 3 | **Cell viability studies.** MB231 cell viability studies 72 h after treatment with 100 nM sp^2-based commercial compounds and bioisostere-containing analogues of (A) *Boscalid*. (B) *Phthalylsulfathiazole*. (C) *Telmisartan*.

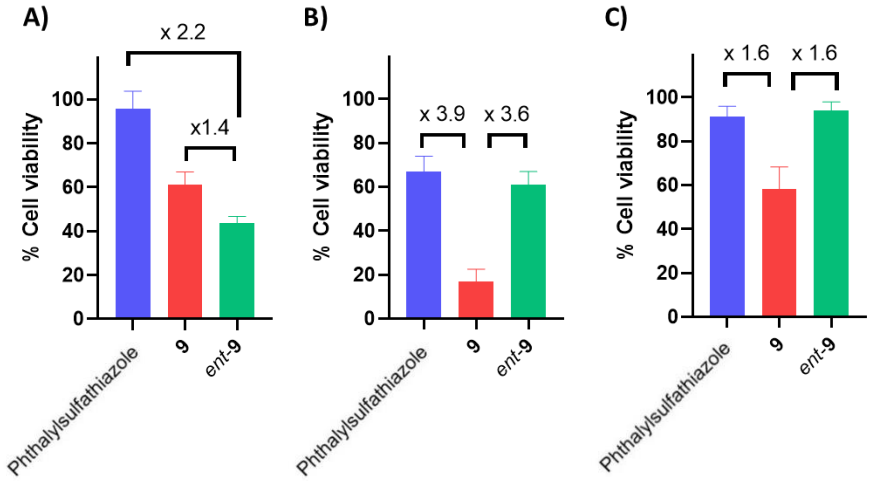

Figure 4 | **Cell viability studies.** Cell viability studies 72 h after treatment with *Phthalylsulfathiazole* and its bioisostere-containing analogues **9** and *ent*-**9**. (A) MB231 treated with 100 nM. (B) Mel202 treated with 200 nM. (C) HCT116 treated with 600 nM.

Mechanistic proposal

In accordance with previously reported activations of unsaturated compounds by the chiral-at-rhodium catalyst,[57] the Lewis acid is establishing an efficient bidentate binding with the acyl pyrazole moiety to give a Lewis acid-substrate complex that can absorb photons under visible light irradiation. As clearly noticeable through observation of the UV-vis absorption spectra of the reaction components (Figure 5a), at the specific wavelength employed for the photoreaction (λ = 440 nm), the unbound substrate **1g** is not capable of any light absorption, avoiding any undesired racemic background reaction. On the other hand, the rhodium catalyst and the reaction mixture composed of the substrate and the catalyst show an absorption in the visible light region. Indeed, an enhanced absorption profile is observed for the reaction mixture solution in comparison with the sole catalyst, indicating that a new species has been formed by coordination of the substrate to the rhodium. Although the unbound catalyst **Λ-RhS** could reach an excited state upon absorption, this species cannot enable any productive reactions and it will revert to its ground state by non-radiative deactivation pathways. Thus, the Lewis acid-substrate complex **Λ-RhS-1g** is the only active species under visible light irradiation. Once the Lewis acid-substrate complex reaches its singlet excited state it will populate its triplet excited state by an expected rapid intersystem crossing (ISC). This triplet excited species can undergo fast *E/Z*-isomerization and eventually carry out a stereocontrolled [2+2] photocycloaddition by a stepwise mechanism (Figure 5b). Indeed, upon the first carbon-carbon bond formation, the obtained triplet diradical species must undergo a further ISC to achieve the ring closure of the cyclobutane by a second bond formation. The absolute configuration observed for the bicyclo[2.1.1]hexane scaffold can be predicted by the proposed Lewis acid-substrate complex model (Figure 5b), and it was investigated by Density Functional Theory (DFT) calculations (Figure 5c and Supporting Information for further details). This allowed us to establish (*i*) which is the Lewis acid-substrate complex that is more likely undergoing a crossed [2+2] photocycloaddition, (*ii*) which is the first cyclobutane bond formed in the process, and (*iii*) how the tethered olefin is approaching the double bond of the α,β-unsaturated acyl

pyrazole, permitting to rationalize the reaction outcome in terms of stereoconvergency, diastereoselectivity and enantioselectivity.

The Lewis acid substrate-complexes of both *E*- and *Z*-isomers with an *s-cis* configuration of the bond connecting the carbonyl moiety to the double bond seem to be suitable intermediates to enable a productive [2+2] photocycloaddition, displaying an appropriate disposition of the substituents in the triplet excited state that would allow a ring closure towards the experimentally observed diastereoisomer. This was corroborated by DFT studies with substrate **1a**. Indeed, upon visible light excitation, the same two triplet species (*s-cis*)-**A** and (*s-cis*)-**A-*ent*** can be obtained regardless of the stereochemistry of the starting double bond (see Figure S105 of the Supplementary Information for further details), allowing the establishment of a fast light-mediated *E/Z*-isomerization. These triplet species present the two unpaired electrons in two different p-orbitals that are perpendicular to each other. Thus, the phenyl and the tethered alkene are perpendicular to the plane of the acyl pyrazole moiety and the excited double bond. The (*s-cis*)-**A** species (phenyl above the plane) is 3.9 kcal/mol more stable than the (*s-cis*)-**A-*ent*** species (phenyl below the plane), very likely as a result of the higher steric congestion between the catalyst *tert*-butyl group and the tethered olefin in the latter complex. The different disposition of the tethered alkene would lead to the formation of the two possible enantiomers of the product: **2a** [via (*s-cis*)-**A**], and **2a-*ent*** [via (*s-cis*)-**A-*ent***], respectively. On the other hand, an alternative (*s-trans*)-**A** complex could be formed, although our calculations indicate that this species is 9.5 kcal/mol less stable than its *s-cis* counterpart in the triplet hypersurface. Due to its high energy, *s-trans* species can be discarded as active Lewis acid-substrate complexes, which explains the lack of any product (*i.e.* the diastereoisomer of **2a**) derived from them.

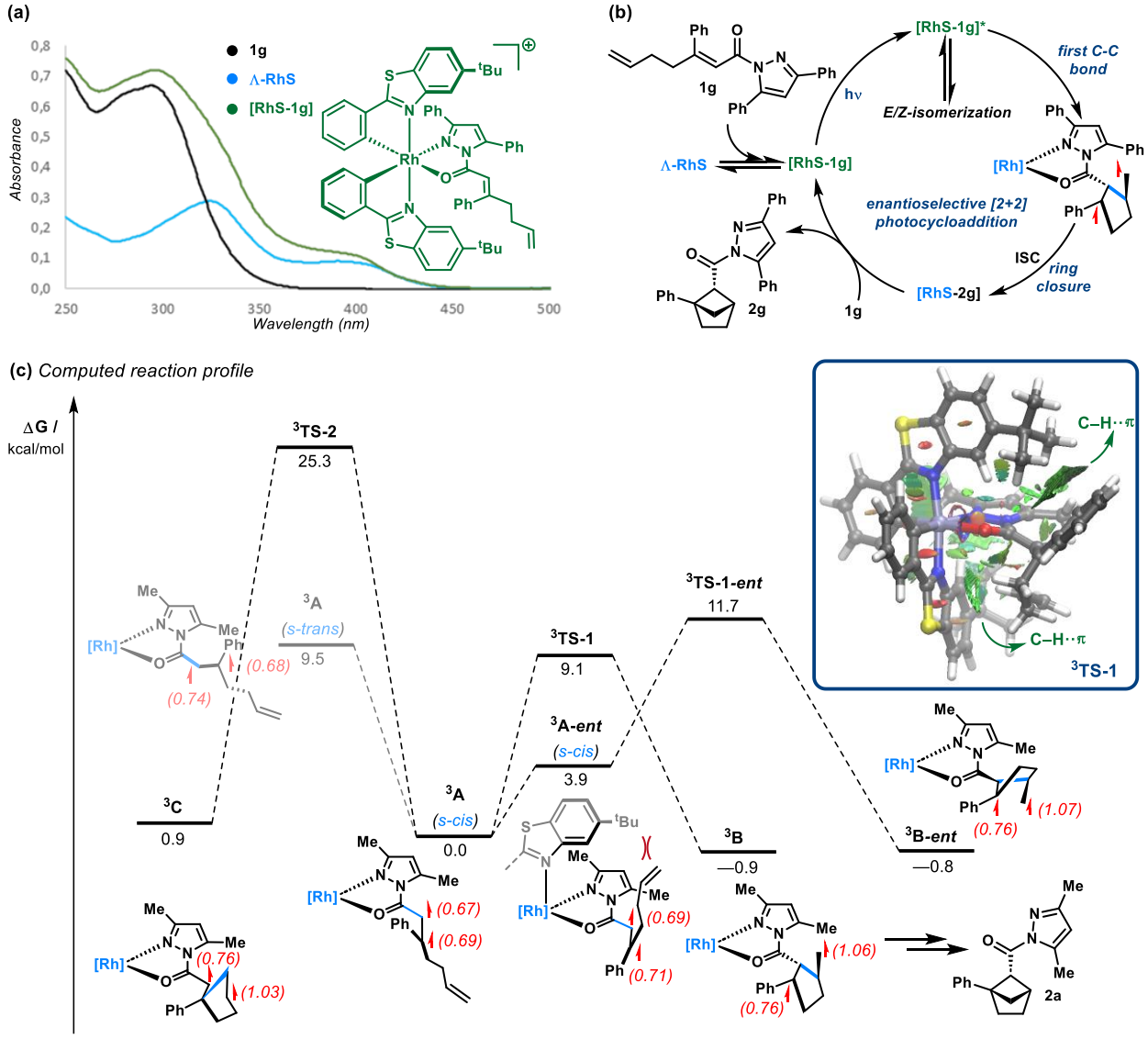

Figure 5 | **(a) UV-vis absorption spectra** (reaction mixture and individual components). **(b) Mechanistic proposal**. **(c) Computed reaction profile** (PCM(acetone)-(u)-B3LYP-D3/def2-TZVPP//PCM(acetone)-(u)B3LYP-D3/def2-SVP level) for the process involving substrate **1a**. Relative free energy values (ΔG, at 298 K) are given in kcal/mol whereas red values within parenthesis indicate the computed spin-densities. Inset: Contour plots of the reduced density gradient isosurfaces (density cutoff of 0.05 a.u.) for ^{3}**TS-1**. The green surfaces indicate attractive non-covalent interactions (see Supporting Information for details).

Moreover, to determine which is the first carbon-carbon bond of the cyclobutane that is formed, we first calculated the Gibbs free energies of the two possible triplet diradical intermediates. As expected, intermediate **^{3}B**, which would originate upon establishment of a carbon-carbon bond between the α-carbonyl carbon and the internal position of the tethered olefin, is 1.8 kcal/mol more stable than intermediate **^{3}C**, which would originate from the alternative ring closing event. This is essentially due to the higher stability of the tertiary benzylic (and primary) diradical **^{3}B** in comparison with the alternative α-carbonyl centered (and secondary) diradical **^{3}C** (see computed spin-densities in Figure 5c). In addition, the pathway leading to **^{3}C** requires a much higher activation barrier than that leading to **^{3}B** ($\Delta\Delta G^{\neq}$ = 16.2 kcal/mol), which renders this alternative cyclization reaction non-competitive. Moreover, due to the presence of bulky *tert*-butyl substituents in the ligand framework of **Λ-RhS**, one of the enantiotopic faces of the α,β-unsaturated acyl pyrazole within the Lewis acid-substrate complex displays an enhanced steric congestion, which leads to a mandatory approximation of the tethered olefin from the other side, enabling the first bond formation. Indeed, upon calculation of the possible transition states associated with the first ring closure, we observed that ^{3}**TS1** has a lower activation barrier in comparison with ^{3}**TS1-*ent***. The computed free energy difference ($\Delta\Delta G^{\neq}$ = 2.6 kcal/mol) is consistent with the almost complete enantioselectivity (*er* = 95:5, see Table 1) observed experimentally. The higher stability of **^{3}TS1** can be attributed not only to unfavorable steric clashes in **^{3}TS1-*ent*** but also to the occurrence of stabilizing C–H···π non-covalent interactions in **^{3}TS-1** (see greenish surfaces in the inset of Figure 5c). It is important to notice that, in this case, once the first bond has been established, the diastereoselectivity and the enantioselectivity of the reaction are fixed, which fully agrees with the exclusive formation of a single diastereoisomer observed experimentally. Indeed, this could not be the case for the alternative triplet diradical species **^{3}C** if dissociation from the catalyst occurs before the cyclobutane ring forms, with the acyl pyrazole moiety assuming a different spatial orientation before ISC.

Conclusions

An asymmetric catalytic strategy to access enantioenriched 1,5-disubstituted bicyclo[2.1.1]hexanes as suitable bioisosteres of *ortho*-substituted phenyl rings has been established. This strategy relies on a Lewis acid-catalyzed intramolecular crossed [2+2] photocycloaddition that works with α,β-unsaturated acyl pyrazoles, providing modulable and versatile products in high yield and enantioselectivity. The utility of these building blocks was showcased by the synthesis of enantioenriched sp^3-analogues of several marketed drugs containing an *ortho*-substituted phenyl ring. The bioactivity of the enantioenriched compounds has been evaluated, and a comparison between the two enantiomers and the sp^2-based structure was done, highlighting that the absolute configuration and tridimensionality of the sp^3-hybridized scaffold has a large impact on it. Particularly, compound **9** presents 3.9-fold higher antitumoral activity compared with its parent drug *Phthalylsulfathiazole*, and what is more, it exhibits a 3.6-fold higher toxicity than *ent*-**9** for the rare cancer uveal melanoma. This study provides a convenient procedure for obtaining enantioenriched saturated bioisosteres as building blocks for medicinal chemistry, allowing their use and implementation in drug discovery programs to prepare analogues with enhanced physicochemical properties and bioactivities.

Acknowledgements

Financial support was provided by the European Commission (ERC Consolidator Grant to M.T. - grant n. 101002715) and the Spanish Ministry of Science and Innovation (MICINN) [grant n. PID2022-142594NB-I00 to M.T, grant n. PID2019-106184GB-I00 and RED2018-102387-T to I.F., grant n. PID2020- 119352RB-I00 to A.S.]. A.S. would like to thank the Spanish Association Against Cancer (AECC), and IMDEA Nanociencia acknowledges support from the Spanish "Severo Ochoa" Programme for Centres of Excellence in R&D (grant n. CEX2020-001039-S). We would like to acknowledge Dr. Josefina Perles (SIdI-UAM) for X-ray structure analysis, and we would like to thank Prof. Dr. José M. Lassaletta and Prof. Dr. Rosario Fernández (Universidad de Sevilla) for allowing us to use their HPLC equipment.

Data availability

Materials and methods, experimental procedures, complete computational details, ^{1}H and ^{13}C NMR spectra, and HRMS data are available in the Supplementary Information. Crystallographic data for compounds **3** and **8** have been deposited with the Cambridge Crystallographic Data Centre under accession codes CCDC 2286648 and 2286647, respectively.

Author contributions

M.T. and T.R. conceived of the project. P.G.-G., I.Q. and T.R. performed the experimental work. P.M-R. and A.S. performed the biological studies. I.F. performed the computational calculations. M.T. and T.R. interpreted the data and wrote the manuscript with input from all authors.

Competing interests

The authors declare no competing interests.

References

1) Taylor, R. D., MacCoss, M. & Lawson, A. D. G. Rings in drugs. *J. Med. Chem.* **57**, 5845–5859 (2014).

2) Buskes, M. J. & Blanco, M.-J. Impact of Cross-Coupling Reactions in Drug Discovery and Development. *Molecules* **25**, 3493 (2020).

3) Meyer, E. A., Castellano, R. K. & Diederich, F. Interactions with aromatic rings in chemical and biological recognition. *Angew. Chem., Int. Ed.* **42**, 1210–1250 (2003).

4) de Freitas R. F. & Schapira, M. A systematic analysis of atomic protein–ligand interactions in the PDB. *Med. Chem. Comm.* **8**, 1970–1981 (2017).

5) Locke, G. M., Bernhard, S. S. R. & Senge, M. O. Nonconjugated hydrocarbons as rigid-linear motifs: isosteres for material sciences and bioorganic and medicinal chemistry. *Chem. Eur. J*. **25**, 4590–4647 (2019).

6) Lovering, F., Bikker, J. & Humblet, C. Escape from Flatland: increasing saturation as an approach to improving clinical success. *J. Med. Chem.* **52**, 6752–6756 (2009).

7) Mykhailiuk, P. K. Saturated bioisosteres of benzene: where to go next? *Org. Biomol. Chem*. **17**, 2839–2849 (2019).

8) Subbaiah, M. A. M. & Meanwell, N. A. Bioisosteres of the phenyl ring: recent strategic applications in lead optimization and drug design. *J. Med. Chem.* **64**, 14046–14128 (2021).

9) Pellicciari, R., Raimondo, M., Marinozzi, M., Natalini, B., Costantino, G., Thomsen, C. (S)-(+)-2-(3‘-Carboxybicyclo[1.1.1]pentyl)-glycine, a structurally new group I metabotropic glutamate receptor antagonist. *J. Med. Chem.* **39**, 2874−2876 (1996).

10) For a recent example of the Mykhailiuk group regarding the synthesis of an ideal *para*-substituted benzene bioisostere, see: Levterov, V. V., Panasyuk, Y., Sahun, K., Stashkevich, O., Badlo, V., Shablykin, O., Sadkova, I., Bortnichuk, L., Klymenko-Ulianov, O., Holota, Y., Bas, J. P., & Mykhailiuk, P. K. An “ideal” bioisoster of the *para*-substituted phenyl ring. *ChemRxiv* (2023) DOI: 10.26434/chemrxiv-2023-rbgz3.

11) Makarov, I. S., Brocklehurst, C. E., Karaghiosoff, K., Koch, G. & Knochel, P. Synthesis of bicyclo[1.1.1]pentane bioisosteres of internal alkynes and *para*-disubstituted benzenes from [1.1.1]propellane. *Angew. Chem. Int. Ed*. **56**, 12774–12777 (2017).

12) Kanazawa, J., Maeda, K. & Uchiyama, M. Radical multicomponent carboamination of [1.1.1]propellane. *J. Am. Chem. Soc.* **139**, 17791–17794 (2017).

13) Zhang, X., Smith, R. T., Le, C., McCarver, S. J., Shireman, B. T., Carruthers, N. I. & MacMillan, D. W. C. Copper-mediated synthesis of drug-like bicyclopentanes. *Nature* **580**, 220–226 (2020).

14) Dong, W., Yen-Pon, E., Li, L., Bhattacharjee, A., Jolit, A. & Molander, G. A. Exploiting the sp^2 character of bicyclo[1.1.1]pentyl radicals in the transition-metal-free multi-component difunctionalization of [1.1.1]propellane. *Nat. Chem.* **14**, 1068–1077 (2022).

15) Yu, I. F., Manske, J. L., Diéguez-Vázquez, A., Misale, A., Pashenko, A. E., Mykhailiuk, P. K., Ryabukhin, S. V., Volochnyuk, D. M. & Hartwig, J. F. Catalytic undirected borylation of tertiary C–H bonds in bicyclo[1.1.1]pentanes and bicyclo[2.1.1]hexanes. *Nat. Chem.* **15**, 685–693 (2023).

16) Yu, S., Jing, C., Noble, A. & Aggarwal, V. K. 1,3-Difunctionalizations of [1.1.1]propellane via 1,2-metallate rearrangements of boronate complexes. *Angew. Chem. Int. Ed*. **59**, 3917–3921 (2020).

17) Ripenko, V., Vysochyn, D., Klymov, I., Zhersh, S. & Mykhailiuk, P. K. Large-scale synthesis and modifications of bicyclo[1.1.1]pentane-1,3-dicarboxylic acid (BCP). *J. Org. Chem.* **86**, 14061−14068 (2021).

18) Nugent, C., Arroniz, C., Shire, B. R., Sterling, A. J., Pickford, H. D., Wong, M. L. J., Mansfield, S. J., Caputo, D. F. J., Owen, B., Mousseau, J. J., Duarte, F. & Anderson, E. A. A general route to bicyclo[1.1.1]pentanes through photoredox catalysis. *ACS Catal*. **9**, 9568–9574 (2019).

19) Pickford, H. D., Ripenko, V., McNamee, R. E., Holovchuk, S., Thompson, A. L., Smith, R. C., Mykhailiuk, P. K. & Anderson, E. A. Rapid and scalable halosulfonylation of strain-release reagents. *Angew. Chem. Int. Ed.* e202213508 (2022).

20) Ripenko, V., Sham, V., Levchenko, V., Holovchuk, S., Vysochyn, D., Klymov, I., Kyslyi, D., Veselovych, S., Zhersh, S., Dmytriv, Y., Tolmachov, A., Sadkova, I., Pishel, I., Mykhailiuk, P. The largest library of bicyclo[1.1.1]pentanes for drug discovery enabled by light. ChemRxiv (2023), DOI: 10.26434/chemrxiv-2023-8dclm.

21) Denisenko, A., Garbuz, P., Shishkina, S. V., Voloshchuk, N. M. & Mykhailiuk, P. K. Saturated bioisosteres of *ortho*-substituted benzenes. *Angew. Chem. Int. Ed.* **59**, 20515–20521 (2020).

22) The Mykhailiuk group recently designed the synthesis of 2-oxabicyclo[2.1.1]hexanes as oxygen-containing analogues of bicyclo[2.1.1]hexanes with improved solubility: Denisenko, A., Garbuz, P., Voloshchuk, N. M., Holota, Y., Al-Maali, G., Borysko, P. & Mykhailiuk, P. K. 2-Oxabicyclo[2.1.1]hexanes as saturated bioisosteres of the *ortho*-substituted phenyl ring. *Nat. Chem.* **15**, 1155–1163 (2023).

23) Zhao, J.-X., Chang, Y.-X., He, C., Burke, B. J., Collins, M. R., Del Bel, M., Elleraas, J., Gallego, G. M., Montgomery, T. P., Mousseau, J. J, Nair, S. K., Perry, M. A., Spangler, J. E., Vantourout, J. C. & Baran, P. S. 1,2-Difunctionalized bicyclo[1.1.1]pentanes: long–sought-after mimetics for *ortho*/*meta*-substituted arenes. *Proc. Natl. Acad. Sci. USA* **118**, e2108881118 (2020).

24) Ma, X., Han, Y. & Bennett, D. J. Selective synthesis of 1-dialkylamino-2-alkylbicyclo-[1.1.1]pentanes. *Org. Lett*. **22**, 9133–9138 (2020).

25) Garry, O. L., Heilmann, M., Chen, J., Liang, Y., Zhang, X., Ma, X., Yeung, C. S., Bennett, D. J. & MacMillan, D. W. C. Rapid access to 2-substituted bicyclo[1.1.1]pentanes. *J. Am. Chem. Soc.* **145**, 3092−3100 (2023).

26) Yang, Y., Tsien, J., Hughes, J. M. E., Peters, B. K., Merchant, R. R. & Qin, T. An intramolecular coupling approach to alkyl bioisosteres for the synthesis of multisubstituted bicycloalkyl boronates. *Nat. Chem.* **13**, 950–955 (2021).

27) Guo, R. Chang, Y.-C., Herter, L., Salome, C., Braley, S. E., Fessard, T. C. & Brown, M. K. Strain release [2π + 2σ] cycloadditions for the synthesis of bicyclo[2.1.1]hexanes initiated by energy transfer. *J. Am. Chem. Soc.* **144**, 7988–7994 (2022).

28) Agasti, S., Beltran, F., Pye, E., Kaltsoyannis, N., Crisenza, G. E. M. & Procter, D. J. A catalytic alkene insertion approach to bicyclo[2.1.1]hexane bioisosteres. *Nat. Chem*. **15**, 535–541 (2023).

29) Liu, Y., Lin, S., Li, Y., Xue, J.-H., Li, Q. & Wang, H. Pyridine-boryl radical-catalyzed [2π + 2σ] cycloaddition of bicyclo[1.1.0]butanes with alkenes. *ACS Catal.* **13**, 5096−5103 (2023).

30) Liang, Y., Kleinmans, R., Daniliuc, C. G. & Glorius, F. Synthesis of polysubstituted 2-oxabicyclo[2.1.1]hexanes via

visible-light-induced energy transfer. *J. Am. Chem. Soc.* **144**, 20207–20213 (2022).

31) Liang, Y., Paulus, F., Daniliuc, C. G. & Glorius, F. Catalytic formal [2π+2σ] cycloaddition of aldehydes with bicyclobutanes: expedient access to polysubstituted 2-oxabicyclo[2.1.1]hexanes. *Angew. Chem. Int. Ed.* e202305043 (2023).

32) Frank, N., Nugent, J., Shire, B. R., Pickford, H. D., Rabe, P., Sterling, A. J., Zarganes-Tzitzikas, T., Grimes, T., Thompson, A. L., Smith, R. C., Schofield, C. J., Brennan, P. E., Duarte, F. & Anderson, E. A. Synthesis of *meta*-substituted arene bioisosteres from [3.1.1]propellane. *Nature* **611**, 721–726 (2022).

33) Iida, T., Kanazawa, J., Matsunaga, T., Miyamoto, K., Hirano, K. & Uchiyama, M. Practical and facile access to bicyclo[3.1.1]heptanes: potent bioisosteres of *meta*-substituted benzenes. *J. Am. Chem. Soc.* **144**, 21848–21852 (2022).

34) Levterov, V. V., Panasyuk, Y., Pivnytska, V. O. & Mykhailiuk, P. K. Water-soluble non-classical benzene mimetics. *Angew. Chem. Int. Ed.* **59**, 7161-7167 (2022).

35) Rigotti, T. & Bach, T. Bicyclo[2.1.1]hexanes by visible light-driven intramolecular crossed [2 + 2] photocycloadditions. *Org. Lett.* **24**, 8821−8825 (2022).

36) Yu, T., Yang, J., Wang, Z., Ding, Z., Xu, M., Wen, J., Xu, L. & Li, P. Selective [2σ + 2σ] cycloaddition enabled by boronyl radical catalysis: synthesis of highly substituted bicyclo[3.1.1]heptanes. *J. Am. Chem. Soc.* **145**, 4304−4310 (2023).

37) Zheng, Y., Huang, W., Dhungana, R. K., Granados, A., Keess, S., Makvandi, M., & Molander, G. A. Photochemical intermolecular [3σ + 2σ]-cycloaddition for the construction of aminobicyclo[3.1.1]heptanes. *J. Am. Chem. Soc*. **144**, 23685−23690 (2022).

38) Epplin, R. C., Paul, S., Herter, L., Salome, C., Hancock, E. N., Larrow, J. F., Baum, E. W., Dunstan, D. R., Ginsburg-Moraff, C., Fessard, T. C. & Brown, M. K. [2]-Ladderanes as isosteres for *meta*-substituted aromatic rings and rigidified cyclohexanes. *Nat. Commun.* **13**, 6056 (2022).

39) Wiesenfeldt, M. P., Rossi-Ashton, J. A., Perry, I. B., Diesel, J., Garry, O. L., Bartels, F., Coote, S. C., Ma, X., Yeung, C. S., Bennett, D. J. & MacMillan, D. W. C. General access to cubanes as benzene bioisosteres. *Nature* **618**, 513–518 (2023).

40) Kazi, N., Aublette, M. C., Allinson, S. L. & Coote, S. C. A practical synthesis of 1,3-disubstituted cubane derivatives. *Chem*. *Commun*. **59**, 7971–7973 (2023).

41) Harmata, A. S., Spiller, T. E., Sowden, M. J. & Stephenson, C. R. J. Photochemical formal (4 + 2)-cycloaddition of imine-substituted bicyclo[1.1.1]pentanes and alkenes. *J. Am. Chem. Soc*. **143**, 21223–21228 (2021).

42) Wright, B. A., Matviitsuk, A., Black, M. J., García-Reynaga, P., Hanna, L. E., Herrmann, A. T., Ameriks, M. K., Sarpong, R. & Lebold, T. P. Skeletal editing approach to bridge-functionalized bicyclo[1.1.1]pentanes from azabicyclo[2.1.1]hexanes. *J. Am. Chem. Soc.* **145**, 10960–10966 (2023).

43) Herter, L., Koutsopetras, I., Turelli, L., Fessard, T. & Salomé, C. Preparation of new bicyclo[2.1.1]hexane compact modules: an opening towards novel sp^3-rich chemical space. *Org. Biomol. Chem.* **20**, 9108–9111 (2022).

44) Smith, E., Jones, K. D., O'Brien, L., Argent, S. P., Salome, C., Lefebvre, Q., Valery, A., Böcü, M., Newton, G. N. & Lam, H. W. Silver(I)-Catalyzed Synthesis of Cuneanes from Cubanes and their Investigation as Isosteres. *J. Am. Chem. Soc.* **145**, 16365−16373 (2023).

45) Son, J.-Y., Aikonen, S., Morgan, N., Harmata, A. S., Sabatini, J. J., Sausa, R. C., Byrd, E. F. C., Ess, D. H., Paton, R. S. & Stephenson, C. R. J. Exploring Cuneanes as Benzene Isosteres and Energetic Materials: Scope and Mechanistic Investigations into Regioselective Rearrangements from Cubanes. *J. Am. Chem. Soc.* **145**, 16355−16364 (2023).

46) Brooks, W. H., Guida, W. C. & Daniel, K. G. The significance of chirality in drug design and development. *Curr. Top. Med. Chem.* **11**, 760–770 (2011).

47) Parra, A., Amenós, L., Guisán-Ceinos, M., López, A., García Ruano, J. L. & Tortosa, M. Copper-catalyzed diastereo- and enantioselective desymmetrization of cyclopropenes: synthesis of cyclopropylboronates. *J. Am. Chem. Soc*. **136**, 15833–15836 (2014).

48) Guisán-Ceinos, M., Parra, A., Martín-Heras, V. & Tortosa, M. Enantioselective synthesis of cyclobutylboronates via a copper-catalyzed desymmetrization approach. *Angew. Chem. Int. Ed.* **55**, 6969–6972 (2016).

49) Nóvoa, L., Trulli, L., Parra, A. & Tortosa, M. Stereoselective diboration of spirocyclobutenes: a platform for the synthesis of spirocycles with orthogonal exit vectors. *Angew. Chem. Int. Ed.* **60**, 11763–11768 (2021).

50) Nóvoa, L., Trulli, L., Fernández, I., Parra, A. & Tortosa, M. Regioselective monoborylation of spirocyclobutenes. *Org. Lett.* **23**, 7434–7438 (2021).

51) Teresa, J.; Velado, M.; Fernández de la Pradilla, R.; Viso, A.; Lozano, B. & Tortosa, M. Enantioselective Suzuki cross-coupling of 1,2-diboryl cyclopropanes. *Chem. Sci*. **14**, 1575-1581 (2023).

52) Stephenson, C. R. J., Yoon, T. P. & MacMillan, D. W. C. *Visible Light Photocatalysis in Organic Chemistry* (Wiley-VCH, 2018).

53) Genzink, M. J., Kidd, J. B., Swords, W. B. & Yoon, T. P. Chiral photocatalyst structures in asymmetric photochemical synthesis. *Chem. Rev.* **122**, 1654–1716 (2022).

54) Poplata, S., Tröster, A., Zou, Y.-Q. & Bach, T. Recent advances in the synthesis of cyclobutanes by olefin [2 + 2] photocycloaddition reactions. *Chem. Rev.* **116**, 9748–9815 (2016).

55) Ojima, I. *Catalytic Asymmetric Synthesis* Ch 3 (Wiley, Hoboken, 3rd edn. 2010).

56) Brenninger, C., Jolliffe J. D. & Bach, T. Chromophore activation of α,β-unsaturated carbonyl compounds and its application to enantioselective photochemical reactions. *Angew. Chem. Int. Ed.* **57**, 14338–14349 (2018).

57) Huang, X. & Meggers, E. Asymmetric photocatalysis with bis-cyclometalated rhodium complexes. *Acc. Chem. Res.* **52**, 833–847 (2019).

58) Ma, J., Zhang, X., Huang, X., Luo, S. & Meggers, E. Preparation of chiral-at-metal catalysts and their use in asymmetric photoredox chemistry. *Nat. Protoc.* **13**, 605–632 (2018).

59) Huo, H., Harms, K. & Meggers, E. Catalytic, enantioselective addition of alkyl radicals to alkenes via visible-light-activated photoredox catalysis with a chiral rhodium complex. *J. Am. Chem. Soc.* **138**, 6936−6939 (2016).

60) Huang, X., Quinn, T. R., Harms, K., Webster, R. D., Zhang, L., Wiest, O. & Meggers, E. Direct visible-light-excited asymmetric Lewis acid catalysis of intermolecular [2+2] photocycloadditions. *J. Am. Chem. Soc.* **139**, 9120–9123 (2017).

61) Huang, X., Li, X., Xie, X., Harms, K., Riedel, R. & Meggers, E. Catalytic asymmetric synthesis of a nitrogen heterocycle through stereocontrolled direct photoreaction from electronically excited state. *Nat. Commun*. **8**, 2245 (2017).

62) Hu, N., Jung, H., Zheng, Y., Lee, J., Zhang, L., Ullah, Z., Xie, X., Harms, K., Baik, M.-H. & Meggers, E. Catalytic asymmetric dearomatization by visible-light-activated [2+2] photocycloaddition. *Angew. Chem. Int. Ed*. **57**, 6242–6246 (2018).

63) Zhang, C., Chen, S., Ye, C.-X., Harms, K., Zhang, L., Houk, K. N. & Meggers, E. Asymmetric photocatalysis by intramolecular hydrogen-atom transfer in photoexcited catalyst–substrate complex. *Angew. Chem. Int. Ed.* **58**, 14462–14466 (2019).

64) Rigotti, T., Schwinger, D. P., Graßl, R., Jandl, C. & Bach, T. Enantioselective crossed intramolecular [2+2] photocycloaddition reactions mediated by a chiral chelating Lewis acid. *Chem. Sci*. **13**, 2378–2384 (2022).

65) CCDC 2286648 (**3**) contains the supplementary crystallographic data. These data can be obtained free of charge at www.ccdc.cam.ac.uk.

66) CCDC 2286647 (**8**) contains the supplementary crystallographic data. These data can be obtained free of charge at www.ccdc.cam.ac.uk.